Available online at www.sciencedirect.com
ScienceDirect
Bioorganic & Medicinal Chemistry Letters 17 (2007) 22–27
Bioorganic & Medicinal Chemistry Letters

Acyclic, orally bioavailable ketone-based cathepsin K inhibitors

David G. Barrett,[a,†] John G. Catalano,[a] David N. Deaton,[a,*] Stacey T. Long,[b] Robert B. McFadyen,[a] Aaron B. Miller,[c] Larry R. Miller,[d] Vicente Samano,[a] Francis X. Tavares,[a] Kevin J. Wells-Knecht,[e,‡] Lois L. Wright[f] and Hui-Qiang Q. Zhou[a]

[a]*Department of Medicinal Chemistry, GlaxoSmithKline, Research Triangle Park, NC 27709, USA*
[b]*Department of World Wide Physical Properties, GlaxoSmithKline, Research Triangle Park, NC 27709, USA*
[c]*Discovery Research Computational, Analytical, and Structural Sciences, GlaxoSmithKline, Research Triangle Park, NC 27709, USA*
[d]*Department of Molecular Pharmacology, GlaxoSmithKline, Research Triangle Park, NC 27709, USA*
[e]*Department of Research Bioanalysis and Drug Metabolism, GlaxoSmithKline, Research Triangle Park, NC 27709, USA*
[f]*Discovery Research Biology, GlaxoSmithKline, Research Triangle Park, NC 27709, USA*

Received 30 August 2006; revised 3 October 2006; accepted 4 October 2006
Available online 17 November 2006

Abstract—Starting from a potent ketone-based inhibitor with poor drug properties, incorporation of P^2–P^3 elements from a ketoamide-based inhibitor led to the identification of a hybrid series of ketone-based cathepsin K inhibitors with better oral bioavailability than the starting ketone.

The function of the CA1 clan proteases, the cysteine cathepsins, has traditionally been assumed to involve degradation of proteins in lysosomes; however, in the last 10 years, research has revealed unique roles for individual family members in bone resorption, antigen presentation and processing, prohormone activation, protease maturation, and hair follicle development.[1] Furthermore, discoveries during the last decade have implicated cathepsins in various pathologies including osteoporosis, rheumatoid arthritis, atherosclerosis, neurodegeneration, and cancer, resulting in accelerated development of inhibitors as potential interventions in these diseases. In light of the mounting evidence of the potential utility of inhibitors of cathepsin K, the major bone matrix degrading protease in osteoclasts, in preventing excess bone resorption, much research has focused on the development of such inhibitors as drugs for the treatment of osteoporosis.[2]

Typically, inhibitors of cathepsins utilize an electrophilic warhead to interact with the active site thiol moiety as well as enzyme recognition motifs to facilitate potency and specificity. SmithKline Beecham researchers have developed ketone-based cathepsin K inhibitors exemplified by compound **1**.[3,4] Although potent (cat K IC_{50} = 7.5 nM), ketone **1** showed moderate to high clearance (C_l = 33 mL/min/kg) and poor oral bioavailability (F = 3.2%) in rats. GlaxoWellcome scientists have described ketoamide-based cathepsin K inhibitors such as **2**.[5] Inhibitor **2** is an even more potent inhibitor (cat K IC_{50} = 0.072 nM) than ketone **1**, as one would expect given the greater electrophilicity of its warhead. It is cleared less rapidly (C_l = 9.6 mL/min/kg) and is more bioavailable (F = 42%) in rats than **1**. In 2000, following the formation of GlaxoSmithKline, these researchers decided to explore the idea of incorporating elements from both inhibitor classes to identify a new ketone-based inhibitor series with potentially improved potency and pharmacokinetic properties.

The strategy involved combining the perceived best elements of each inhibitor series in the formation of a hybrid inhibitor. Ketone **1** and ketoamide **2** were modeled[6] into the active site of cathepsin K based on the ketone (1BGO)[7] and ketoamide (1YT7)[5] X-ray

Keywords: Cathepsin K; Cysteine protease inhibitor; Osteoporosis; Electrophilic warhead.
* Corresponding author. Tel.: +1 919 483 6270; fax: +1 919 315 0430; e-mail: david.n.deaton@gsk.com
† Present address: Lilly Forschung GmbH, Essener Str. 93, 22419 Hamburg, Germany.
‡ Present address: Schering-Plough Research Institute, 2015 Galloping Hill, Kenilworth, NJ 07033, USA.

0960-894X/$ - see front matter © 2006 Elsevier Ltd. All rights reserved.
doi:10.1016/j.bmcl.2006.10.102

co-crystal structures (Brookhaven Protein Data Bank) as shown in Figure 1. The model of ketone **1** and ketoamide **2** reveals significant overlap between the two inhibitors. The *i*-butyl moiety of ketone **1** and the *tert*-butyl group of ketoamide **2** both occupy the S^2 pocket, with the benzofuran element of ketone **1** and the 3-phenyl pyrazole component of ketoamide **2** in the substrate trough pointing toward the S^3 subsite, and the methyl and *n*-butyl of ketone **1** and ketoamide **2**, respectively, in the S^1 trough. The major differences between these two inhibitors arise from different modes of attack by the active site thiol on the electrophilic warheads. The cysteine thiol attacks the ketone **1** from the *Si* face inserting the hydroxyl of the thiohemiketal into the oxyanion hole, while the ketoamide is approached from the opposite face placing the amide into the oxyanion hole. Despite this difference the two P^1 groups, the pyridine of ketone **1** and the pyrazole of ketoamide **2** occupy similar space. Given this similarity, it was surmised that the P^2–P^3 groups of the two inhibitors could be interchanged.

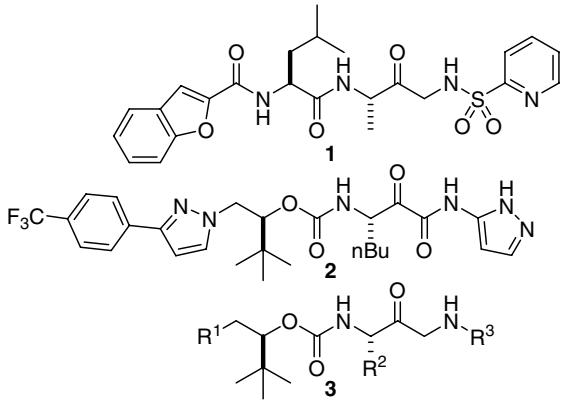

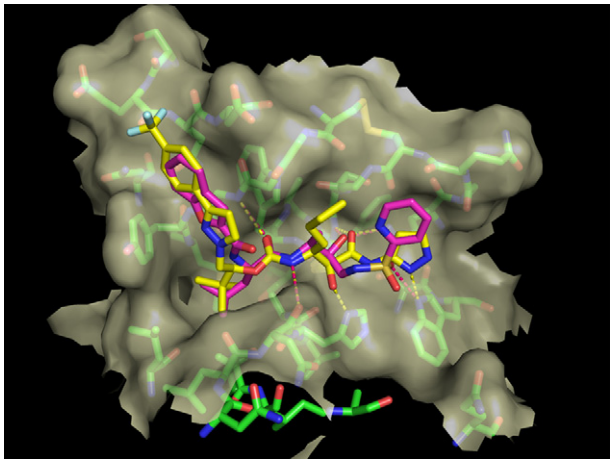

Figure 1. An overlay of ketone **1** and ketoamide **2** docked into the active site of the X-ray structure of cathepsin K based on X-ray co-crystal structures of similar ketones (1BGO) and ketoamides (1YT7). The cathepsin K carbons are colored green with inhibitor **1** carbons colored magenta and inhibitor **2** carbons colored yellow. The semi-transparent gray surface represents the molecular surface, while hydrogen bonds are depicted as yellow/red dashed lines. This figure was generated using PYMOL version 0.99 (Delano Scientific, www.pymol.org).

The ketone, although inherently less electrophilic and therefore less potent, was chosen as the warhead for the hybrid because it might interact with fewer nucleophilic moieties in vivo, and thereby potentially produce fewer side effects during chronic therapy.[8] Furthermore, hypothesizing that the presence of two amide bonds in inhibitor **1** contributed to its high clearance, it was surmised that replacement of these fragments with the P^2–P^3 carbamate element of inhibitor **2** would afford a hybrid ketone series **3** with enhanced metabolic stability and improved pharmacokinetics relative to the starting ketone.[9]

The ketone analogs **3a**–**m** were prepared as depicted in Scheme 1. The known aldehydes **4b** (R^2 = Me) and **4c** (R^2 = *n*-Bu) were converted to their corresponding cyanohydrins under acidic catalysis, then the nitriles were reduced to provide the amines **5b** and **5c** as mixtures of hydroxyl epimers.[10] The alcohol **5a** (R^2 = H) has previously been disclosed.[11] Alcohols **7a**–**e** were prepared by reacting amines **5a** and **5b** with sulfonyl chloride **6a** or amine **5c** with sulfonyl chloride **6a**, carbamoyl chloride **6b**, or difluoropyridine **6c**, respectively. Then, acid catalyzed cleavage of the *tert*-butyl carbamate protecting group afforded amines which were coupled with the known *para*-nitrophenyl carbonates **8a**–**g** to provide the carbamates **9a**–**m**.[12] Finally, Dess–Martin oxidation of the secondary alcohols **9a**–**m** produced the desired ketones **3a**–**m**.

As shown in Table 1, the hybrid analogs **3a**–**m** that contain the ketone electrophile of inhibitor **1** and the P^2 *tert*-butyl carbamate of ketoamide **2** are potent cathepsin K inhibitors, many of which show similar activity to the starting ketone **1**. A quick study of the structure–activity relationships of the S^1 wall of cathepsin K revealed that the P^1 *n*-Bu moiety of **3c** (IC_{50} = 4.0 nM) is apparently more potent than the P^1 hydrogen

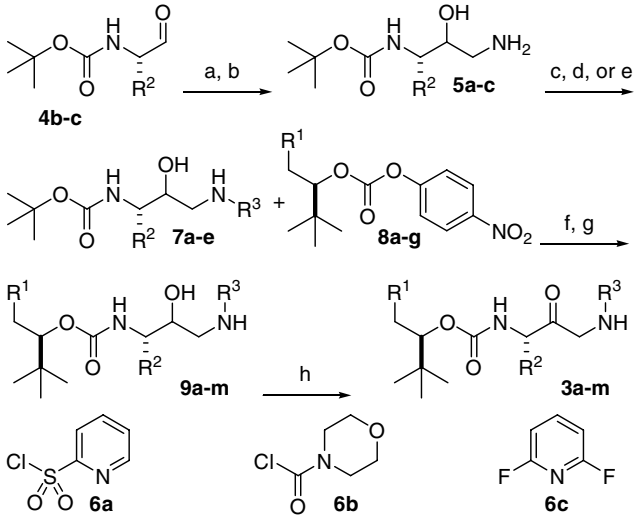

Scheme 1. Reagents: (a) KCN, HOAc, MeOH; (b) H_2/PtO_2–C, HOAc, 46%; (c) **5a**–**5c**, **6a**, CH_2Cl_2, $NaHCO_3$, H_2O, 34–65%; (d) **5c**, **6b**, *i*-Pr_2NEt, CH_2Cl_2, 89%; (e) **5c**, **6c**, *i*-Pr_2NEt, dioxane, 29%; (f) HCl, dioxane, 99%; (g) **8a**–**g**, *i*-Pr_2NEt, DMF, 45–93%; (h) Dess–Martin periodinane, CH_2Cl_2, $NaHCO_3$, 15–68%.

Table 1. Inhibition of human cathepsin K

Compound	R^1	R^2	R^3	IC_{50}[a] (nM)
1				7.5
2				0.072
3a	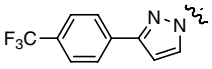	H	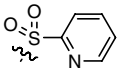	65
3b	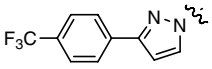	Me	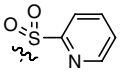	18
3c	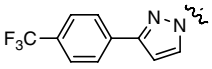	*n*-Bu	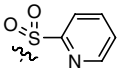	4.0
3d	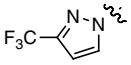	Me	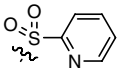	300
3e	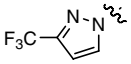	*n*-Bu	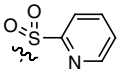	32
3f	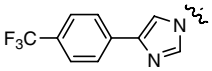	*n*-Bu	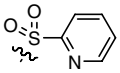	6.4
3g	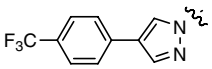	*n*-Bu	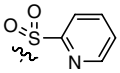	7.6
3h	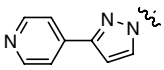	*n*-Bu	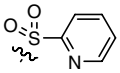	3.8
3i	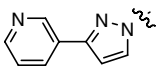	*n*-Bu	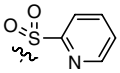	5.5
3j	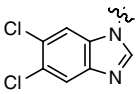	Me	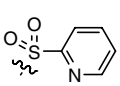	1.4
3k	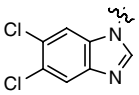	*n*-Bu	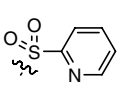	3.2
3l	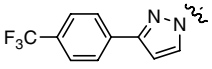	*n*-Bu	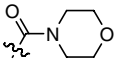	>250
3m	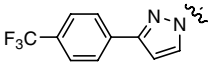	*n*-Bu	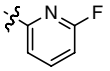	2.1

[a] Inhibition of recombinant human cathepsin K activity in a fluorescence assay using 10 μM Cbz-Phe-Arg-AMC as substrate in 100 mM NaOAc, 10 mM DTT, and 120 mM NaCl, pH 5.5. The IC_{50} values are the mean of two or three inhibition assays, individual data points in each experiment were within a threefold range of each other.

analog **3a** (IC_{50} = 65 nM) and the P^1 methyl analog **3b** (IC_{50} = 18 nM) (compare also **3d** to **3e**). A similar P^1 SAR trend was also seen in the ketoamide series exemplified by inhibitor **2**.[13]

In addition to the exploration of the S^1 groove of the enzyme, the S^3 subsite of cathepsin K was also investigated in the hybrid ketone series. Truncation of the P^3 group by removing the terminal phenyl ring as in analogs **3d** (IC_{50} = 300 nM) and **3e** (IC_{50} = 32 nM) resulted in a 5- to 10-fold loss in activity (compare **3d** to **3b** or **3e** to **3c**), presumably arising from reduced interactions with the S^3 subsite of the enzyme. In contrast, the nature of the five-membered aryl spacer between P^2 and P^3 did not greatly influence the inhibitory activity within this series. For example, the pyrazole **3c** (IC_{50} = 4.0 nM), imidazole **3f** (IC_{50} = 6.4 nM), and isomeric pyrazole **3g** (IC_{50} = 7.6 nM) were equipotent cathepsin K inhibitors. Apparently, this structural element serves mainly to orient the P^3 group toward the S^3 subsite as well as to enhance the aqueous solubility of the inhibitor. Altering the electronics of this conformational constraint has little effect on inhibitor potency. Since cathepsin K contains a carboxylic acid group (^{61}Asp) in its S^3 subsite, analogs with a complementary charge in P^3 were also explored to try to form an ionic bond with the acidic S^3 element.[14] Both of the isomeric pyridyl derivatives **3h** (IC_{50} = 3.8 nM) and **3i** (IC_{50} = 5.5 nM) were equipotent to the neutral phenyl analog **3c** despite the higher entropic cost paid by these analogs to desolvate the

Table 2. Cathepsin B, L, and S inhibition and selectivity

Compound	Cat K IC_{50} (nM)	Cat B IC_{50} [a] (nM)	Cat L IC_{50} [b] (nM)	Cat S IC_{50} [c] (nM)
1	7.5	59	—	20
2	0.072	20	8.7	0.21
3b	18	310	>250	64
3c	4.0	170	>250	35
3f	6.4	130	1100	10
3g	7.6	72	7100	26
3h	3.8	13	38	11
3i	5.5	79	100	15
3j	1.4	71	38	7.9
3k	3.2	40	16	10
3m	2.1	68	>250	19

[a] Inhibition of recombinant human cathepsin B activity in a fluorescence assay using 10 μM Cbz-Phe-Arg-AMC as substrate in 100 mM NaOAc, 10 mM DTT, and 120 mM NaCl, pH 5.5.
[b] Inhibition of recombinant human cathepsin L activity in a fluorescence assay using 5 μM Cbz-Phe-Arg-AMC as substrate in 100 mM NaOAc, 10 mM DTT, and 120 mM NaCl, pH 5.5.
[c] Inhibition of recombinant human cathepsin S activity in a fluorescence assay using 10 μM Cbz-Val-Val-Arg-AMC as substrate in 100 mM NaOAc, 10 mM DTT, and 120 mM NaCl, pH 5.5.

Table 3. Serum pharmacokinetics of hybrid ketone analogs

Compound	*c*log *P*	MDCK P_{APP} (nm/s)	Sol. FS-SIF[a] (mg/mL)	$t_{1/2}$ [b] (min)	C_l [c] (mL/min/kg)	V_{SS} [d] (mL/kg)	*F* [e] (%)
1	3.4	—	—	33	33	710	3.2
2	5.5	91	0.11	320	9.6	1600	42
3b	5.6	300	0.097	32	82	1800	27
3c	7.2	160	0.041	120	26	1800	21
3e	3.7	340	—	24	21	460	20
3f	6.8	190	0.040	67	47	1600	22
3h	4.9	68	0.060	120	16	1700	100
3k	7.0	150	0.028	46	31	1300	32

[a] FS-SIF is the equilibrium solubility in fasted state-simulated intestinal fluid at pH 6.8. The values are the mean of two measurements.
[b] $t_{1/2}$ is the iv terminal half-life dosed as a solution in male Han Wistar rats. All in vivo pharmacokinetic values are the mean of two experiments.
[c] C_l is the total clearance.
[d] V_{SS} is the steady-state volume of distribution.
[e] *F* is the oral bioavailability when dosed as a solution.

pyridine moiety relative to the phenyl group upon binding to the enzyme. This suggests that the pyridines do indeed form a charge complex with the carboxylic acid of ^{61}Asp in cathepsin K, but that the enthalpic gain is offset by the entropic cost of desolvation. Although potency was not enhanced, aqueous solubility should be increased, potentially leading to improved oral absorption. Interestingly, incorporation of the particularly potent P^3 benzimidazole group from the ketoamide series into the hybrid ketone series afforded mixed results. The benzimidazole group was more potent in the P^1 methyl analog **3j** (compare **3j** IC_{50} = 1.4 nM to **3b**), but not the P^1 *n*-butyl analog **3k** (compare **3k** IC_{50} = 3.2 nM to **3c**).

After investigating the S^3 subsite of cathepsin K with various P^3 probes, a brief study of the carboxy-terminal substrate binding region of the enzyme was pursued. The $P^{1'}$ morpholinocarbamate analog **3l** showed little inhibition at concentrations up to 250 nM. In contrast, the fluoropyridyl derivative **3m** (IC_{50} = 2.1 nM) was equipotent with the pyridylsulfonamide **3c**. This result suggested that further efforts in the $P^{1'}$ region might prove fruitful; however, for strategic reasons further

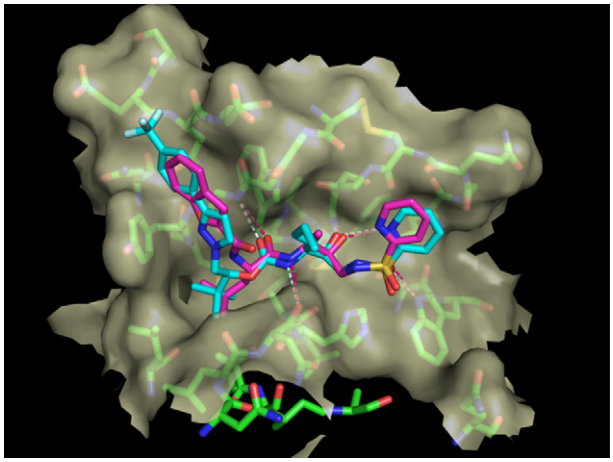

Figure 2. An overlay of ketone **1** and ketone **3c** docked into the active site of the X-ray structure of cathepsin K based on X-ray co-crystal structure of a similar ketone (1BGO). The cathepsin K carbons are colored green with inhibitor **1** carbons colored magenta and inhibitor **3c** carbons colored cyan. The semi-transparent gray surface represents the molecular surface, while hydrogen bonds are depicted as white/red dashed lines. This figure was generated using PYMOL version 0.99 (Delano Scientific, www.pymol.org).

exploration of this hybrid ketone series was not undertaken.

Similar to the ketoamide series, these hybrid ketones showed moderate to good selectivity versus cathepsin L (e.g., analogs **3f**, **3g**, and **3m** $\geqslant$100-fold selective for cathepsin K), as shown in Table 2. In contrast, these hybrid ketones were substantially less selective than the corresponding ketoamides against cathepsin B (only ~10-fold selective for cathepsin K).[5] Their selectivity versus cathepsin S was poor.

These ketones exhibited good to excellent permeability in an in vitro Madin-Darby canine kidney (MDCK) cell permeation assay (P_{APP} = 68–340 nm/s), as shown in Table 3.[15] Furthermore, their solubility in fasted state-simulated intestinal fluid (FS-SIF = 0.028–0.097 mg/mL) at pH 6.8 was only slightly lower than that of ketoamide **2** (FS-SIF 0.11 mg/mL), which exhibited good oral exposure.[16] Encouraged by these predictors of oral bioavailability, the iv and po pharmacokinetics of several analogs were profiled in male Han Wistar rats. As shown in Table 3, the compounds exhibited short terminal elimination half-lives ($t_{1/2}$ = 24–120 min) and moderate to high clearances (C_l = 16–82 mL/min/kg), similar to starting ketone **1** ($t_{1/2}$ = 33 min, C_l = 33 mL/min/kg). In contrast, the steady-state volumes of distribution (V_{SS} = 460–1800 mL/kg) on average resembled the more moderate volume of starting ketoamide **2** (V_{SS} = 1600 mL/kg) than ketone **1** (V_{SS} = 710 mL/kg). Encouragingly, the oral bioavailabilities (F = 20–100%) of the hybrid ketones were all significantly better than that of the starting ketone **1** (F = 3.2%), with the 4-pyridyl derivative **3h** (F = 100%) exhibiting similar oral and intravenous exposure.

A model of the hybrid ketone **3c** docked into the active site of cathepsin K with the active site thiol of ^{25}Cys forming a covalent hemithioketal intermediate with the ketone group of the inhibitor is shown in Figure 2. The model of starting ketone **1** is included for comparison. This model provides insight into the SAR of the hybrid ketone series. The hemithioketal hydroxyl of ketone **3c** is stabilized by two hydrogen bonds to the side chain of ^{19}Gln, and the backbone amide of ^{25}Cys, consistent with other ketone co-crystal structures (e.g., 1BGO). One face of the P^1 *n*-butyl group of the norleucine-derived inhibitor forms van der Waals interactions with the S^1 wall composed of ^{23}Gly, ^{24}Ser, ^{64}Gly, and ^{65}Gly. Moreover, the carbamate NH and the carbamate carbonyl of the inhibitor are stabilized by two additional hydrogen bonds between ^{161}Asn and ^{66}Gly in the peptide backbone recognition site of the enzyme. Furthermore, the P^2 *tert*-butyl substituent of **3c** forms significant lipophilic interactions with the deep S^2 pocket composed of ^{67}Tyr, ^{68}Met, ^{134}Ala, ^{163}Ala, and ^{209}Leu. Additional interactions between the P^3 phenyl moiety and the active site trough as well as the S^3 subsite formed by ^{60}Asn, ^{61}Asp, ^{65}Gly, ^{66}Gly, and ^{67}Tyr further enhance binding energy. Finally, the pyridyl sulfonamide occupies the $S^{1'}$ subsite with one of its sulfone oxygens forming a hydrogen bond with the indole NH of ^{184}Trp. The hybrid ketone **3c** and the starting ketone **1** occupy very similar space reflective of their similar potencies.

In summary, this report describes the design of a novel hybrid ketone series of cathepsin K inhibitors based on two previously disclosed cathepsin K inhibitor series. Significant enhancements in oral exposure were realized by eliminating two amide bonds and incorporating a constrained P^3 peptidomimetic fragment, while maintaining the low nanomolar inhibitory activity of the original ketone versus cathepsin K. Further efforts to improve the selectivity of this series versus other cathepsins via modifications to the P^3 residue may prove worthwhile.

Acknowledgments

The authors thank Robert Marquis and Dennis Yamashita for helpful discussions.

References and notes

1. Turk, B.; Turk, D.; Salvesen, G. S. *Med. Chem. Rev.-Online* **2005**, *2*, 283.
2. Deaton, D. N.; Kumar, S. *Prog. Med. Chem.* **2004**, *42*, 245.
3. Marquis, R. W.; Ru, Y.; LoCastro, S. M.; Zeng, J.; Yamashita, D. S.; Oh, H.-J.; Erhard, K. F.; Davis, L. D.; Tomaszek, T. A.; Tew, D.; Salyers, K.; Proksch, J.; Ward, K.; Smith, B.; Levy, M.; Cummings, M. D.; Haltiwanger, R. C.; Trescher, G.; Wang, B.; Hemling, M. E.; Quinn, C. J.; Cheng, H. Y.; Lin, F.; Smith, W. W.; Janson, C. A.; Zhao, B.; McQueney, M. S.; D'Alessio, K.; Lee, C.-P.; Marzulli, A.; Dodds, R. A.; Blake, S.; Hwang, S.-M.; James, I. E.; Gress, C. J.; Bradley, B. R.; Lark, M. W.; Gowen, M.; Veber, D. F. *J. Med. Chem.* **2001**, *44*, 1380.
4. Marquis, R. W.; Ward, K. W.; Roethke, T.; Smith, B. R.; Ru, Y.; Yamashita, D. S.; Tomaszek, T. A.; Gorycki, P. D.; Cheng, H. Y.; James, I. E.; Stroup, G. B.; Lark, M. W.; Gowen, M.; Veber, D. F. *Mol. Pharm.* **2004**, *1*, 97.
5. Barrett, D. G.; Boncek, V. M.; Catalano, J. G.; Deaton, D. N.; Hassell, A. M.; Jurgensen, C. H.; Long, S. T.; McFadyen, R. B.; Miller, A. B.; Miller, L. R.; Payne, J. A.; Ray, J. A.; Samano, V.; Shewchuk, L. M.; Tavares, F. X.; Wells-Knecht, K. J.; Willard, D. H.; Wright, L. L.; Zhou, H.-Q. Q. *Bioorg. Med. Chem. Lett.* **2005**, *15*, 3540.
6. Lambert, M. H. In *Practical Application of Computer-Aided Drug Design*; Charifson, P. S., Ed.; Marcel Dekker, NY: New York, 1997; p 243.
7. DesJarlais, R. L.; Yamashita, D. S.; Oh, H.-J.; Uzinskas, I. N.; Erhard, K. F.; Allen, A. C.; Haltiwanger, R. C.; Zhao, B.; Smith, W. W.; Abdel-Meguid, S. S.; D'Alessio, K.; Janson, C. A.; McQueney, M. S.; Tomaszek, T. A.; Levy, M. A.; Veber, D. F. *J. Am. Chem. Soc.* **1998**, *120*, 9114.
8. Jones, D. M.; Atrash, B.; Teger-Nilsson, A.-C.; Gyzander, E.; Deinum, J.; Szelke, M. *Lett. Pept. Sci.* **1995**, *2*, 147.
9. Whitman, D. B.; Askew, B. C.; Duong, L. T.; Fernandez-Metzler, C.; Halczenko, W.; Hartman, G. D.; Hutchinson, J. H.; Leu, C.-T.; Prueksaritanont, T.; Rodan, G. A.; Rodan, S. B.; Duggan, M. E. *Bioorg. Med. Chem. Lett.* **2004**, *14*, 4411.
10. Catalano, J. G.; Deaton, D. N.; Furfine, E. S.; Hassell, A. M.; McFadyen, R. B.; Miller, A. B.; Miller, L. R.;

Shewchuk, L. M.; Willard, D. H.; Wright, L. L. *Bioorg. Med. Chem. Lett.* **2004**, *14*, 275.
11. Kinney, W. A.; Abou-Gharbia, M.; Garrison, D. T.; Schmid, J.; Kowal, D. M.; Bramlett, D. R.; Miller, T. L.; Tasse, R. P.; Zaleska, M. M.; Moyer, J. A. *J. Med. Chem.* **1998**, *41*, 236.
12. Deaton, D. N.; Catalano, J. G. PCT Int. Appl. WO 2003031437, 2003; . *Chem. Abstr.* **2003**, *138*, 304173.
13. Tavares, F. X.; Boncek, V.; Deaton, D. N.; Hassell, A. M.; Long, S. T.; Miller, A. B.; Payne, A. A.; Miller, L. R.; Shewchuk, L. M.; Wells-Knecht, K.; Willard, D. H., Jr.; Wright, L. L.; Zhou, H.-Q. *J. Med. Chem.* **2004**, *47*, 588.
14. Somoza, J. R.; Palmer, J. T.; Ho, J. D. *J. Mol. Biol.* **2002**, *322*, 559.
15. Irvine, J. D.; Takahashi, L.; Lockhart, K.; Cheong, J.; Tolan, J. W.; Selick, H. E.; Grove, J. R. *J. Pharm. Sci.* **1999**, *88*, 28.
16. Dressman, J. B.; Amidon, G. L.; Reppas, C.; Shah, V. P. *Pharm. Res.* **1998**, *15*, 11.